To cite this article: HU X Q, HUANG Z, LIU Z H. Numerical analysis on bending-torsional coupling stiffness characteristics of composite propeller [J/OL]. Chinese Journal of Ship Research, 2022, 17(1). http://www.ship-research.com/en/article/doi/10.19693/j.issn.1673-3185.02224.

DOI: 10.19693/j.issn.1673-3185. 02224

Numerical analysis on bending-torsional coupling stiffness characteristics of composite propeller

HU Xiaoqiang, HUANG Zheng, LIU Zhihua*

College of Naval Architecture and Ocean Engineering, Naval University of Engineering, Wuhan 430033, China

Abstract: [**Objectives**] The bending-torsional coupling deformation degree of a composite propeller reflects the stiffness characteristics of the blade, which in turn have a certain correlation with its hydrodynamic performance. A fiber layer design for a composite propeller is optimized from the perspective of stiffness. [**Method**] Taking a DTMB 4383 composite propeller as the research object, based on the self-iterative algorithm of the fluid-structure interaction of the composite propeller, a numerical calculation method for the bending stiffness and torsional stiffness of the blade is constructed. The stiffness of the blade under different layer schemes is numerically calculated under the conditions of unidirectional carbon fiber cloth or orthogonal carbon fiber cloth laid on the blade, and the bending-torsional stiffness characteristics of the blade and its corresponding laws with hydrodynamic performance are studied. [**Results**] The numerical calculation results show that the thrust coefficient of the single blade, the difference value of the thrust coefficient of the composite propeller, and the stiffness of the blade exhibit relatively synchronous change laws; under the same elastic modulus in the main direction, the minimum difference value of the thrust coefficient of the composite propeller with orthogonal carbon fiber cloth is greater than that with unidirectional carbon fiber cloth; when the elastic modulus of the material decreases, the stiffness of the blade decreases, and the thrust coefficient of the single blade and the difference value of the thrust coefficient of the composite propeller also decreases; when the stiffness of the blade is small, the composite propeller can give fuller play to the advantages of the adaptive flow field, and the bending-torsional coupling produces larger pitch deformation, resulting in a smaller periodic thrust ripple than that of a metal propeller in the high and low flow areas. [**Conclusion**] The results of this paper can guide the optimization design of composite propellers by improving the hydrodynamic performance of the stern.

Key words: composite propeller; bending stiffness; torsional stiffness; thrust coefficient; difference value of thrust coefficient

CLC number: U664.33; U661.1

0 Introduction

Due to the anisotropic mechanical properties of composite materials, the composite propeller will undergo complex bending-torsional coupling deformation under the hydrodynamic load of the flow field. Through the reasonable layer lay-up design of the blade, the composite propeller can realize favorable bending-torsional coupling deformation under the effect of fluid-structure coupling, thus adapting to the flow field and having better hydrodynamic performance. The bending-torsional coupling deformation of the composite propeller includes bending and torsional deformations, and the degree of deformation reflects the stiffness characteristics of the blade. Furthermore, there is a correlation between the stiffness characteristics of the blade and its hydrodynamic performance, and thus the study on such correlation can provide a basis for the lay-up design.

Received: 2020 − 12 − 15 **Accepted**: 2021 − 03 − 09

Supported by: National Natural Science Foundation of China (51179198)

Authors: HU Xiaoqiang , male, born in 1993, master degree candidate. Research interest: hydrodynamic performance of the ship. E-mail: 987693397@qq.com

HUANG Zheng, male, born in 1989, Ph.D., lecturer. Research interest: hydrodynamic performance of the ship. E-mail: huangzheng.315@163.com

***Corresponding author**: HUANG Zheng

In the study on stiffness characteristics of the composite blade, Niu et al.[1-3] took the maximum displacement of the blade as the index of blade stiffness. Although it is relatively intuitive to characterize and analyze the stiffness qualitatively by the maximum displacement, it is difficult to reflect the deformation characteristics of the blade in bending and torsion by the displacement variation alone. Because of the complex bending-torsional coupling deformation of the composite blade, it is necessary to quantify the bending and torsional deformation. In terms of wind turbine blades, studies on their bending-torsional coupling deformation characteristics are also carried out. Wang [4] reflected the bending and torsional deformation characteristics of the wind turbine blade by studying the vibration mode; He [5] characterized the bending deformation in axial and circumferential directions by the maximum deformation of the blade and the torsional deformation of the blade by the variation in the pitch angle of blade tip during the fluid-structure coupling analysis of the composite propeller; Su et al. [6] tested the bending and torsional deformation of the engine blade by experiment. All these studies show that the bending-torsional stiffness of the blade is the embodiment of composite material anisotropy and blade geometric complexity, and the calculation of the bending and torsional stiffness is an important step for studying their performance effects. However, these previous studies which reflect the blade stiffness by the maximum bending and torsional deformation fail to consider the gradual changes of the flow field pressure and the bending and torsional deformation, and cannot reveal the relationship between the bending force and bending deformation, as well as the relationship between the torsional moment and torsional deformation. Because there is a correlation between the blade stiffness and its hydrodynamic performance, the exploration of numerical methods for calculating the bending and torsional stiffness of the blade can help to optimize the fiber layer design of the composite propeller from the perspective of stiffness to improve the hydrodynamic performance and realize the scheme design of the composite propeller.

Therefore, for the bending-torsional coupling deformation characteristics of the composite propeller, this paper studies the self-iterative algorithm for the fluid-structure coupling of the composite propeller with DTMB 4383 composite propeller as the research object, and then calculates the bending-torsional stiffness of the blade with different layer lay-up schemes under the two cases of unidirectional or orthogonal carbon fiber cloth in an attempt to study the bending-torsional stiffness characteristics of the blade and the correspondence law between the bending-torsional stiffness characteristics and the hydrodynamic performance.

1 Self-iterative algorithm for fluid-structure coupling of composite propeller

1.1 Calculation of hydrodynamic performance of stiff propeller

The hydrodynamic performance of a stiff propeller is calculated through the panel method based on the perturbation velocity potential. In other words, the method is based on the potential flow theory, and the flow field where the object is located is considered as inviscid with the ideal fluid incompressible, and the entire flow field has a perturbation velocity potential due to the propeller. The blade, hub, and trailing vortex sheet are discretized into several hyperbolic quadrilateral panels, and the center of each panel is considered as the control point. According to the nature of the fundamental solution to the potential flow field, at all control points of the panels on the object surface, both the source sink and dipole are laid out and at the trailing vortex sheet, the dipole is laid out. Furthermore, the perturbation velocity potential $\varphi(p)$ at the point P (x, y, z) on the object surface satisfies the following integral equation:

$$2\pi\varphi(p) = \iint\!\!\!\!\!\!\diagup_{S_b} \left[\varphi \frac{\partial}{\partial n}\left(\frac{1}{r}\right) - \frac{1}{r}\frac{\partial \varphi}{\partial n}\right] \mathrm{d}S + \iint_{S_w} \Delta\varphi \frac{\partial}{\partial n}\left(\frac{1}{r}\right) \mathrm{d}S \tag{1}$$

where $\iint\!\!\!\!\!\!\diagup$ is the Cauchy principal value integral; S_b is the object surface consisting of the blade and hub; S_w is the tail vortex sheet; n is the normal direction of the object surface; r is the distance between the field point and the source point; φ is the intensity density of the dipole distribution on the object surface; $\frac{\partial \varphi}{\partial n}$ is the intensity density of the source distribution on the object surface; $\Delta\varphi$ is the intensity density of the dipole distribution on the trailing vortex sheet; S is the area of the hyperbolic quadrilateral panel.

Under the constraints of impenetrable surface, zero perturbation velocity at infinity, and boundary

conditions such as the isobaric Kutta condition, the first-order partial derivative of the perturbation velocity potential is evaluated to obtain the perturbation velocity at each control point, and then the Bernoulli equation is used to calculate the pressure distribution on the blade surface. Finally, the thrust and torque are corrected for viscous resistance by the modified formula in Reference [7].

In this paper, the open water performance of five propellers—DTMB 4118, DTMB 4119, DTMB 4381, DTMB 4382, and DTMB 4383, is calculated via the panel method program, and the calculated and test values of thrust coefficient K_T and torque coefficient K_Q are shown in Table 1. In comparison with the test data in References [8-9], it is found that in the whole calculation, the maximum errors of the thrust coefficient and the torque coefficient are 7.69% and 11.04%, respectively, and their average errors are 2.05% and 3.29%, respectively. The maximum errors of the two coefficients occur at the advance coefficient of J = 1.0, which is due to the small hydrodynamic calculation results at this advance coefficient, thus magnifying the relative errors of calculation. It has been verified that the calculated values are in good agreement with the test ones in this paper, which indicates that the calculation of hydrodynamic performance of the stiff propeller in this paper has high accuracy.

1.2 Finite element calculation of composite propeller

In this paper, the finite element analysis software ABAQUS is used to establish the finite element model and the loading pressure distribution of the composite propeller by importing the INP file to calculate the structural deformation. The paper also uses the panel method to divide the upper and lower surfaces of the blade into 20 × 20 panels, and the three-dimensional (3D) coordinates of the panel grid points are output to the INP file. The 8-node hexahedral linear incompatible mode cell is selected, and the 3D coordinates of the panel grid points correspond to that of the structural cell node according to the 3D cell coding rules of ABAQUS. Then the command statements for the model construction and pressure loading are written in the INP file. Young [10], through calculation, found that there was a slight difference in terms of calculation results of dividing one-layer or multi-layer cells along the thickness direction. In order to control the number of cells and accelerate the convergence of the fluid-structure coupling calculation, only one layer of cells is set along the thickness direction of the blade in this paper, with the entire blade divided into 400 cells. The propeller blade root is set as a boundary condition of fixed support, and properties of the composite material are set. ABAQUS/Standard is used to solve the INP file, and the deformation field of the composite blade grid points is calculated and output. The finite element model of the blade is shown in Fig.1, and the fiber lay-up angle of the fiber cloth is shown in Fig.2. In Fig.2, x-y is the local coordinate system defining the lay-up directions with the x-axis being the reference direction of the fiber. In this paper, the reference direction of the fiber is set to coincide with the propeller reference line, and the y-axis is the direction perpendicular to the fiber reference direction; θ refers to the fiber layer angle which is positive in the counterclockwise direction.

Table 1 Comparison of open water performance of five propellers

	J = 0.5		J = 0.7		J = 0.833		J = 0.9		J = 1.0	
	K_T	$10K_Q$	K_T	$10K_Q$	K_T	$10K_Q$	K_T	$10K_Q$	K_T	$10K_Q$
DTMB 4118 calculated value	0.277 1	0.455 2	0.203 6	0.361 2	0.151 8	0.292 2	0.124 6	0.255 2	0.082 6	0.197 1
DTMB 4118 test value	0.287 6	0.481 4	0.200 0	0.360 0	–	–	0.123 3	0.244 4	0.076 7	0.177 5
DTMB 4119 calculated value	0.274 9	0.438 7	0.200 0	0.348 4	0.146 9	0.278 7	0.119 0	0.240 3	0.075 9	0.178 7
DTMB 4119 test value	0.285 0	0.477 0	0.200 0	0.360 0	0.146 0	0.280 0	0.120 0	0.239 0	–	–
DTMB 4381 calculated value	0.372 5	0.666 8	0.292 2	0.560 5	0.234 3	0.478 8	0.203 7	0.433 9	0.155 8	0.362 0
DTMB 4381 test value	0.385 0	0.665 0	0.298 0	0.550 0	–	–	0.205 0	0.412 0	0.152 0	0.335 0
DTMB 4382 calculated value	0.392 1	0.668 2	0.306 1	0.555 8	0.246 3	0.472 2	0.215 1	0.427 0	0.167 2	0.355 1
DTMB 4382 test value	0.394 0	0.680 0	0.310 0	0.565 0	–	–	0.215 0	0.435 0	0.165 0	0.360 0
DTMB 4383 calculated value	0.398 9	0.695 6	0.309 5	0.587 5	0.249 1	0.508 5	0.218 1	0.466 0	0.170 9	0.398 8
DTMB 4383 test value	0.385 0	0.662 0	0.310 0	0.570 0	–	–	0.218 0	0.465 0	0.183 0	0.406 0

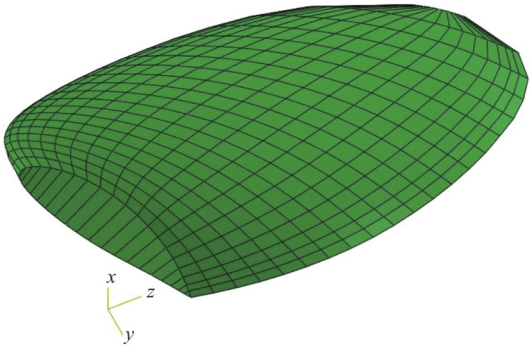

Fig. 1 Finite element model of the blade

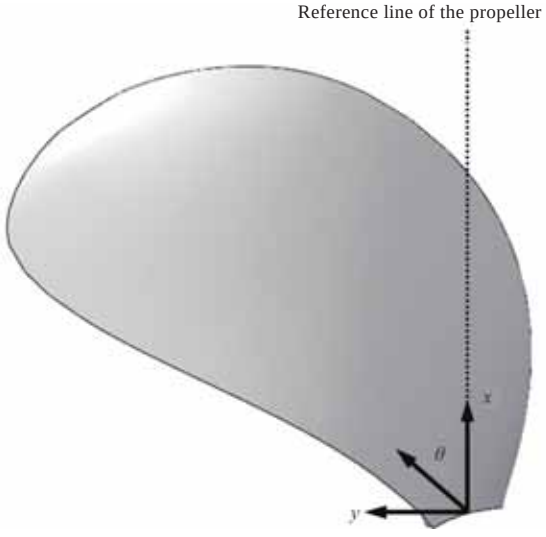

Fig. 2 Fiber layer angle of fiber cloth

1.3 Self-iterative solution of fluid-structure coupling deformation of composite propeller

The self-iterative algorithm takes the panel method program as the main control program and uses the Python scripting language to start a secondary development of the post-processing of ABAQUS to realize the automatic iterative calculation of fluid-structure coupling of the composite propeller. The iterative convergence condition is set as follows: for all grid points of the blade in the last three steps, the difference of their total displacements is less than 0.01 times the propeller diameter, and the initial step of the iteration is set to 4. When the convergence is stable, the hydrodynamic performance and deformation field calculated via fluid-structure coupling are output. The detailed calculation process of fluid-structure coupling is shown in Fig.3.

In this paper, the numerical calculation of the bi-directional fluid-structure coupling is carried out for a carbon fiber composite propeller via the fluid-structure coupling self-iterative program written in this paper. When the advance coefficient J = 0.5–1.0, the convergence of the total displacements at all grid points of the blade is shown in Table 2, and it can be seen that the convergence is achieved in 4 steps of iteration. After the convergence is stable, the calculation results of the thrust coefficient and torque coefficient of fluid-structure coupling are compared with the test results, as shown in Fig. 4. According to the calculation, the average errors of the thrust coefficient and the torque coefficient are 2.94% and 2.49%, respectively, and both of them are controlled within 3%, which verifies that the self-iterative algorithm of the fluid-structure coupling has high accuracy.

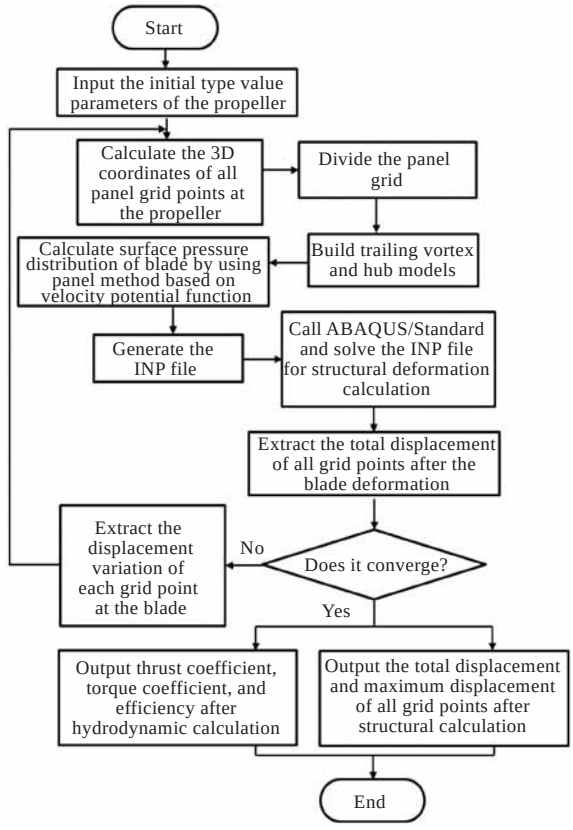

Fig. 3 Fluid-structure coupling calculation process

2 Analysis of stiffness characteristics of composite propeller

The composite propellers will undergo elastic deformation under hydrodynamic loads, which in turn

Table 2 Convergence process of composite propeller

Numbers of iteration	Total displacement of all grid points at the blade/mm					
	J = 0.5	J = 0.6	J = 0.7	J = 0.8	J = 0.9	J = 1.0
0	353.748	310.279	267.339	225.281	183.683	142.428
1	355.414	312.001	268.646	225.787	183.060	140.397
2	355.676	312.230	268.844	225.951	183.191	140.493
3	355.743	312.290	268.895	225.993	183.224	140.518
4	355.760	312.304	268.908	226.004	183.232	140.525

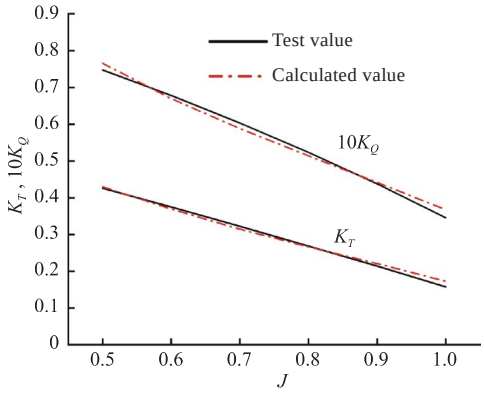

Fig.4 Comparison of the open water performance of carbon fiber composite propeller

affects their hydrodynamic performance. The deformation field changes gradually, and the hydrodynamic power and deformation fields are different in different blades, so the stiffness calculation is required to quantify the deformation capacity of the composite propeller. Young et al.[11] believed that the bending and torsional deformation capacity of the composite propeller are the main factors affecting the hydrodynamic performance, and it is also found in this paper that the influence of composite propeller deformation on hydrodynamic performance is mainly reflected in two aspects: Bending deformation and torsional deformation, which will be calculated and analyzed in the following text.

2.1 Equation for blade stiffness calculation

The study of He[5] showed that the tilting and trim have much less effect on hydrodynamic performance compared with screw pitch, and the effect of trim is reflected in the fluid-structure coupling performance of a large tilting propeller. The variation of the tilting angle reflects the circumferential bending deformation of the blade, but for a marine propeller with a small aspect ratio, such circumferential bending deformation is at a low degree. Therefore, the circumferential bending deformation of the blade will be ignored in this paper, and only the axial bending deformation will be considered. In this paper, the trim variation of the blade is used to characterize the axial bending deformation and the pitch angle variation is used to characterize the torsional deformation; the corresponding force is the thrust force and torsional moment generated by the fluid on the blade, and the stiffness of the blade is calculated by the correlation between such deformation and force.

The equation of the blade's bending stiffness k_1 is as follows:

$$k_1 = \frac{T}{\Delta x} \tag{2}$$

where T is the thrust force of the blade, N; Δx is the trim variation of the blade, mm.

The equation of the blade's torsional stiffness k_2 is as follows:

$$k_2 = \frac{M}{\Delta \beta} \tag{3}$$

where M is the torsional moment of the blade, N·m; $\Delta\beta$ is the pitch angle variation of the blade, (°).

Assume the pitch angle of the blade section at a certain radius of the blade in the initial state is β, and the chord length and the trim are C and $x_{\mathrm{m}}(r)$, respectively. After the blade is deformed, the coordinates of the leading and trailing edges of the blade section at that radius are x'_{l}, y'_{l}, z'_{l} and x'_{t}, y'_{t}, z'_{t}, respectively, and its pitch angle and trim angle become β' and $x'_{\mathrm{m}}(r)$, respectively. According to the geometric relationship, the following equations are deduced.

$$x'_{\mathrm{l}} = x'_{\mathrm{m}}(r) - \frac{C\sin\beta'}{2} \tag{4}$$

$$x'_{\mathrm{t}} = x'_{\mathrm{m}}(r) + \frac{C\sin\beta'}{2} \tag{5}$$

By combining Eqs. (4) and (5), the trim and pitch angles of the deformed blade can be expressed as:

$$x'_{\mathrm{m}}(r) = \frac{x'_{\mathrm{l}} + x'_{\mathrm{t}}}{2} \tag{6}$$

$$\beta' = \arcsin\frac{x'_{\mathrm{t}} - x'_{\mathrm{l}}}{C} \tag{7}$$

The propeller blade is subjected to hydrodynamic loads distributed continuously along its surface under the flow field, and the total effect will put the blade under the torsional moment, which causes the torsional deformation of the blade. Li et al.[12] calculated the centrifugal torsional moment of a controllable pitch propeller with the propeller reference line as the torsional axis, but this torsional moment was mainly used to evaluate the strength of the hub pitching mechanism. Ducoin et al.[13-14] found that the pressure center of the elastic hydrofoil blade section would move from near the midpoint of the nose-tail line toward the leading edge as the angle of attack of the water flow gradually increased from zero. For the propeller blade section, the angle of attack of the flow changes with the change in the advance coefficient, and the pressure center of each blade section will move. Furthermore, if the pressure center moves beyond a threshold, it will change the direction of the torsional moment of the blade section around the midpoint of the chord length. For the composite propeller, such a torsional moment is the root cause of the change in the pitch

of the blade section, which results in a continuous pitch deformation in each blade section. No matter how the angle of attack of the water flow changes, the DTMB 4383 composite propeller blade with large tilting will always suffer from the torsional moment in the negative direction if the propeller reference line is regarded as the torsional axis, and it is not easy to reflect the correlation between the moment of the blade and its torsional deformation. Therefore, the torsional moment of the blade section at each radius of the blade will be calculated separately in this paper, and a line passing through the midpoint of the blade section and parallel to the propeller reference line is considered as the torsional axis at each radius. The positive direction of the torsional moment is shown in Fig.5. In the figure, R refers to the radius of the propeller.

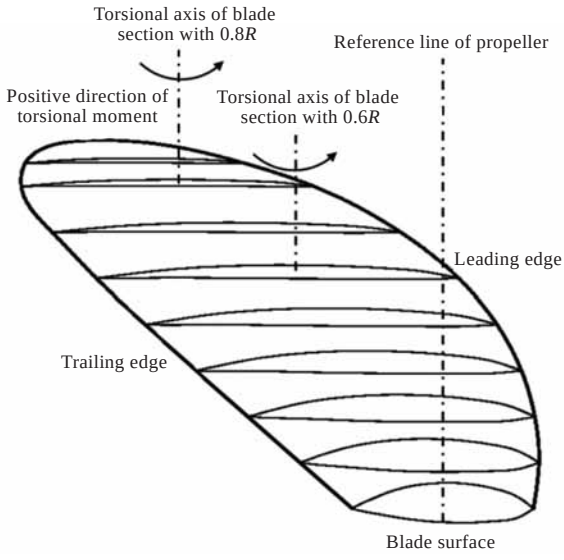

Fig. 5 Schematic diagram of torsional moment in positive direction

In this paper, the total torsional moment of the blade is solved through the "panel discretization and numerical integration". The specific steps are as follows: The upper and lower surfaces of the blade are separated into 20×20 panels, and the resultant force F at each panel control point is decomposed into the component forces F_x, F_y and F_z in three directions along the x, y and z axes of the propeller's rectangular coordinate system. In the coordinate system, the component force F_y does not produce a torsional moment because it is parallel to the torsional axis. The torsional moments tolerated by all the panel are superimposed to get the total torsional moment of the blade.

2.2 Stiffness calculation of unidirectional carbon fiber cloth blade

In this paper, the diameter of the DTMB 4383 composite propeller is 0.304 8 m, and the rotational speed is 25 s^{-1}. In addition, the designed advance coefficient is 0.889. Carbon fiber/resin matrix composite is chosen for Material 1 and Material 2, and the properties of Material 1 [15] are shown in Table 3. The elasticity modulus of Material 2 is half of that of Material 1, as shown in Table 4. In the tables, E_1, E_2, and E_3 refer to the Young's modulus of the material in the directions 1, 2, and 3, respectively; G_{12}, G_{13}, and G_{23} refer to the shear modulus of the material in the planes 1-2, 1-3, and 2-3, respectively. Furthermore, ν_{12}, ν_{13}, and ν_{23} refer to the Poisson's ratio of the material in the planes 1-2, 1-3, and 2-3, respectively. The fiber cloth is laid from the pressure plane of the blade to the suction plane. The fibers of the unidirectional carbon fiber cloth are all oriented in one direction and connected by a braided, and their elasticity modulus in the primary direction is several times that of the two secondary directions. Therefore, the material has clear directivity with the forward fiber angle θ shown in Fig. 2. A total of 12 fiber layer schemes are set in an interval of 15° from −75° to 90°. The calculated operating conditions are chosen near the design ones, i.e., J = 0.7, 0.738, 0.8, 0.889, and 0.9 for a total of five working conditions.

He [5] used the deformation at the blade tip of the

Table 3 The property of Material 1

Parameters	Values
E_1/GPa	165
E_2, E_3/GPa	8.28
G_{12}, G_{13}/GPa	4.27
G_{23}/GPa	2.8
ν_{12}, ν_{13}	0.33
ν_{23}	0.48

Table 4 The property of Material 2

Parameters	Values
E_1/GPa	82.5
E_2, E_3/GPa	4.14
G_{12}, G_{13}/GPa	2.135
G_{23}/GPa	1.4
ν_{12}, ν_{13}	0.33
ν_{23}	0.48

composite propeller to characterize the deformation of the blade. The average value of the deformation of each blade section at 7 radii (0.4R, 0.5R, ..., 0.99R) is chosen to characterize the deformation of the blade in view of the gradient of the pressure in the flow field and the gradient of the blade bending and torsional deformation. It is calculated that there is a difference in the torsional deformation of the composite propeller between the deformation of the tip pitch angle $\Delta\beta_{\mathrm{tip}}$ and the average value of the deformation of each blade section $\Delta\bar{\beta}$. In the case of Material 1, under different operating conditions of all layer schemes, the pitch angle deformation of the DTMB 4383 composite propeller blade is calculated with the above two characterization methods, and the results are shown in Fig. 6 to Fig. 8. From Fig. 6, it can be seen that the pitch angle deformation of the blade tip improves or reduces with the increase of the advance coefficient, and has different patterns. Furthermore, Fig. 7 shows that there is no linear relationship between the pitch angle deformation of the blade tip and the advance coefficient when the fiber angle equals −30°. According to Fig.8, the absolute value of the pitch angle deformation of each blade section in all fiber layer schemes drops with the increase in the advance coefficient, and there is an approximately linear relationship between the pitch angle deformation and the advance coefficient. In comparison, the relationship between the average value of pitch angle deformation of each blade section and the advance coefficient is more regular.

Then, the torsional moment M, the average value of trim deformation of each blade section $\Delta\bar{x}_{\mathrm{m}}$ and the blade thrust T in all fiber layer schemes are calculated, and the results are shown in Figs.9−11. According to the figures, there are approximately linear relationships between torsional moment and advance coefficient, the average value of trim deformation of each blade section and advance coefficient, and propeller thrust and advance coefficient. It can be inferred mathematically that there is an approximately linear relationship between torsional moment and the average value of pitch angle deformation of each blade section and between the average value of blade thrust and trim deformation of

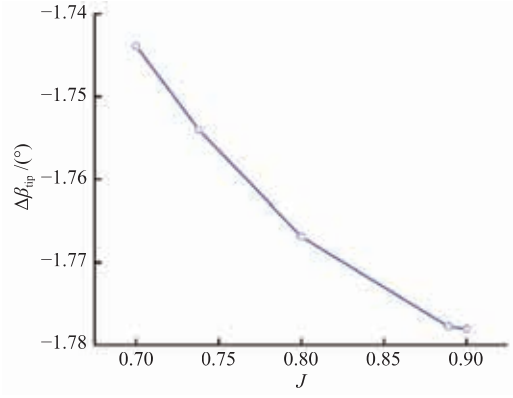

Fig.7 Deformation of pitch angle of blade tip with fiber angle at −30°

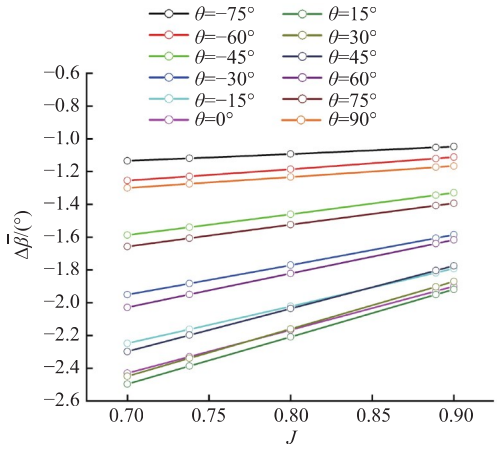

Fig. 8 Average value of pitch angle deformation of each blade section in all fiber layer schemes

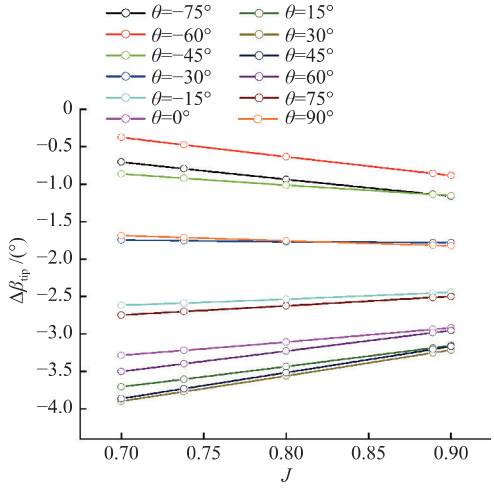

Fig.6 Deformation of pitch angle of blade tip in all fiber layer schemes

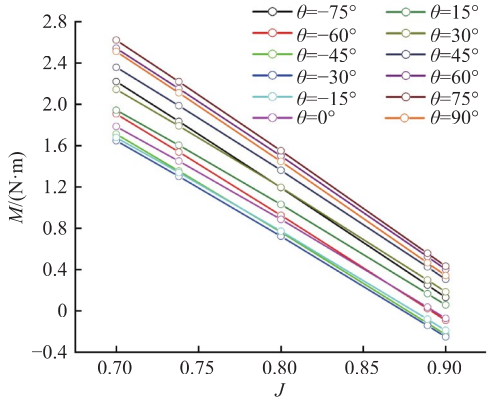

Fig. 9 Torsional moment of blade in all fiber layer schemes

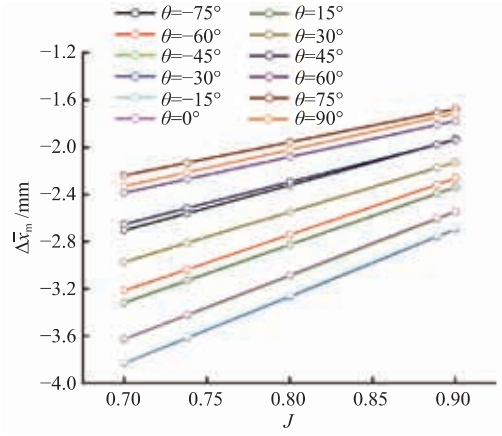

Fig.10 Average value of trim deformation of each blade section in all fiber layer schemes

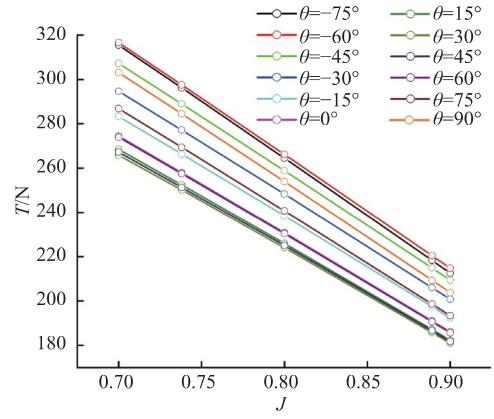

Fig.11 Blade thrust in all fiber layer schemes

each blade section.

According to the linear relationship between the torsional moment and the pitch angle deformation, and between the thrust and the trim deformation, under the adjacent advance coefficient, the absolute value of the first-order difference ratio between the torsional moment and the pitch angle deformation is used to calculate the torsional stiffness of the blade, and that between the thrust and the trim variation is used to calculate the bending stiffness of the blade. The calculation results of the bending and torsional stiffness in the different intervals of advance coefficient under all fiber lay-up schemes are shown in Fig. 12 and Fig. 13, respectively. It can be seen that the torsional and bending stiffness have certain retention around the design condition, and the results of stiffness show good differentiation in terms of the layer angle. In other words, the calculation method of the stiffness can reflect the bending-torsional coupling deformation capability of the specific composite propeller, and it is feasible to study the performance with stiffness as the analysis variable. The calculation results of the stiffness from each advance coefficient interval are averaged as the stiffness of the blade under different fiber lay-up schemes when the blade is laid with Material 1, as shown in Fig. 14. According to the figure, the bending and torsional stiffness of the blade decrease and then increase as the fiber angle of the unidirectional carbon fiber cloth changes from negative to positive, and the changes of both stiffness are basically synchronized, with the minimum bending stiffness and minimum torsional stiffness at a fiber angle of −15° and 15°, respectively. The same method is used for Material 2 in calculating the stiffness, and the results under different fiber layer schemes are shown in Fig. 15. It can be seen that the bending and torsional stiffness of the blade have the same macroscopic trend when the elasticity modulus is halved, but the difference is that the torsional stiffness is smallest at a fiber angle of −15°, which is caused by the complexity of the blade geometry.

2.3 Stiffness calculation of blade with orthogonal carbon fiber cloth

The orthogonal carbon fiber cloth is made of carbon fiber bundles woven vertically in both warp and weft directions. The elasticity modulus of the orthogonal carbon fiber cloth is the same in the two main directions perpendicular to each other in the plane and is several times higher than that in the

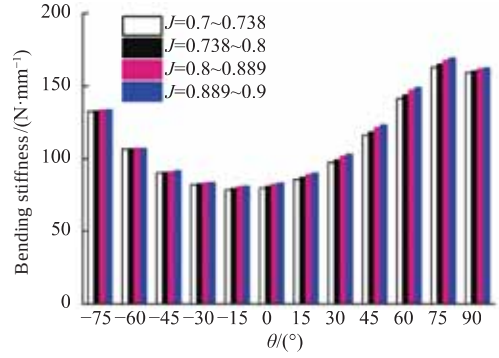

Fig.12 Bending stiffness of blade under different advance coefficient intervals in all fiber layer schemes

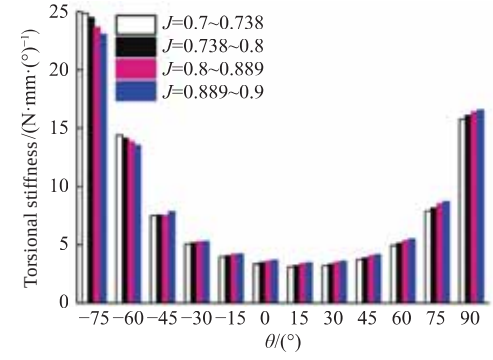

Fig.13 Torsional stiffness of blade under different advance coefficient intervals in all fiber layer schemes

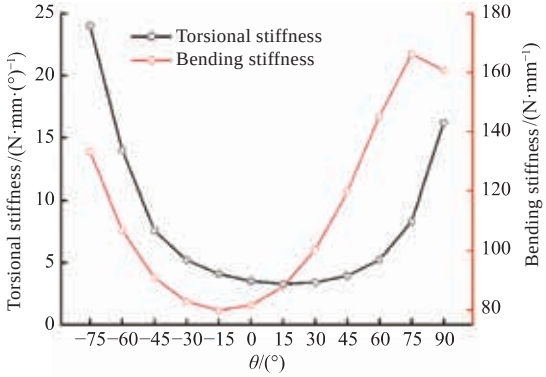

Fig.14 Bending-torsional stiffness of blade under different fiber layer schemes with Material 1

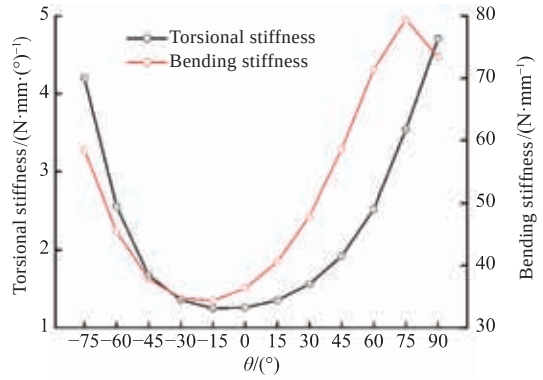

Fig.15 Bending-torsional stiffness of blade under different fiber layer schemes with Material 2

secondary direction. The directivity of the material is symmetric in the plane, which can improve the in-plane strength by avoiding the disadvantage that the unidirectional carbon fiber cloth is subjected to force in only one direction. In this paper, the orthogonal carbon fiber cloth follows the engineering elastic constants of the unidirectional carbon fiber cloth, and two different material properties are adopted. The properties of Material 3 are shown in Table 5, and the elasticity modulus of Material 4 is half of that of Material 3, as shown in Table 6.

The lay-up angle of the orthogonal carbon fiber cloth ranges from 0° to 75°, and six fiber lay-up schemes are set in an interval of 15°. With the above stiffness calculation method, the stiffness of Material 3 and Material 4 are shown in Fig.16 and Fig.17, respectively.

Table 5 The property of Material 3

Parameters	Values
E_1, E_2/GPa	165
E_3/GPa	8.28
G_{12}/GPa	4.27
G_{13}, G_{23}/GPa	2.8
ν_{12}	0.33
ν_{13}, ν_{23}	0.48

Table 6 The property of Material 4

Parameters	Values
E_1, E_2/GPa	82.5
E_3/GPa	4.14
G_{12}/GPa	2.135
G_{13}, G_{23}/GPa	1.4
ν_{12}	0.33
ν_{13}, ν_{23}	0.48

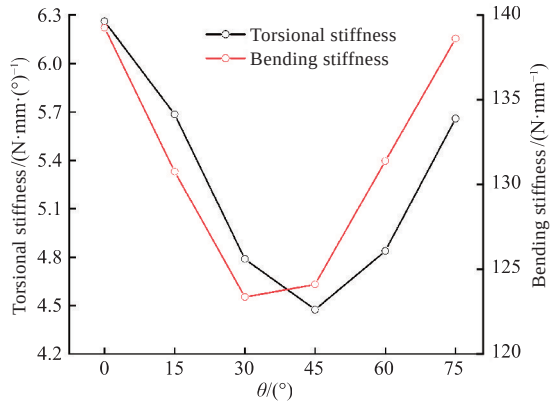

Fig.16 Bending-torsional stiffness of blade under different fiber layer schemes with Material 3

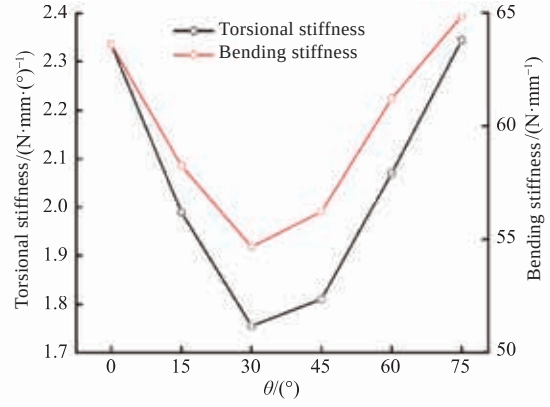

Fig.17 Bending-torsional stiffness of blade under different fiber layer schemes with Material 4

According to Fig. 16 and Fig. 17, it can be seen that the bending stiffness and torsional stiffness of the blade tend to drop and then rise as the fiber angle of the orthogonal carbon fiber cloth gradually increases, and both trends are synchronized. The bending stiffness is the smallest at a fiber angle of 30°, and the torsional stiffness of Material 3 is the smallest at a fiber angle of 45°. When the elasticity modulus is halved, the torsional stiffness of Material 4 is the smallest at a fiber angle of 30°, and such a subtle difference is also caused by the complexity of the blade geometry.

3 Influence rule of blade stiffness on thrust coefficient

The bending-torsional coupling deformation of the composite propeller exposed to hydrodynamic load results in a change in the thrust coefficient. The variation of the blade stiffness and thrust coefficient of the DTMB 4383 composite propeller with the fiber angle under the design condition is given in Figs. 18-21. According to these figures, it can be seen that for the DTMB 4383 composite propeller with large tilting, the thrust coefficient of the blade is smaller than that of the metal blade for both the unidirectional and orthogonal carbon fiber cloths. When the fiber angle of the unidirectional carbon fiber cloth changes from negative to positive, or when the fiber angle of the orthogonal carbon fiber cloth improves gradually, the thrust coefficient and stiffness of the composite propeller blade tend to decrease first and then increase, and both trends are basically synchronized. Compared with the bending stiffness, the torsional stiffness and thrust coefficient are better synchronized. When the elasticity modulus of the material decreases, the blade stiffness of the composite propeller drops, and the thrust coefficient of the blade also declines. The reason is that the small blade stiffness is accompanied by the weaker resistance to deformation and the great torsional deformation and pitch change under the hydrodynamic load, and this further exacerbates the change in its thrust coefficient.

4 Influence rule of blade stiffness on difference value of thrust coefficient

When the propeller works in the non-uniform wake flow field, the top of the propeller disc will be in the high wake flow area, and the bottom of the disc will have a relatively low wake flow effect. Furthermore, the blade enters the high and low wake flow areas above and below the stern in turn, and the circumferential change in the wake flow will cause the thrust ripple of the propeller. Scholars around the world found that one of the advantages of the composite propeller is that it can adapt itself to the flow field and reduce the thrust ripple

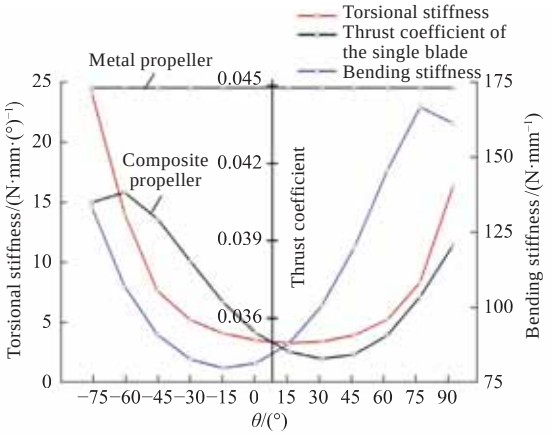

Fig. 18 Bending-torsional stiffness and thrust coefficient of blade with Material 1

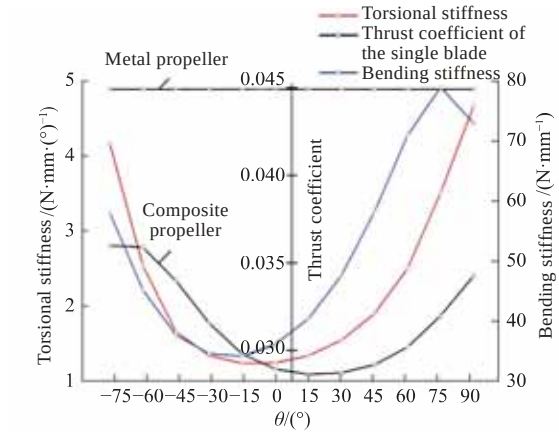

Fig. 19 Bending-torsional stiffness and thrust coefficient of blade with Material 2

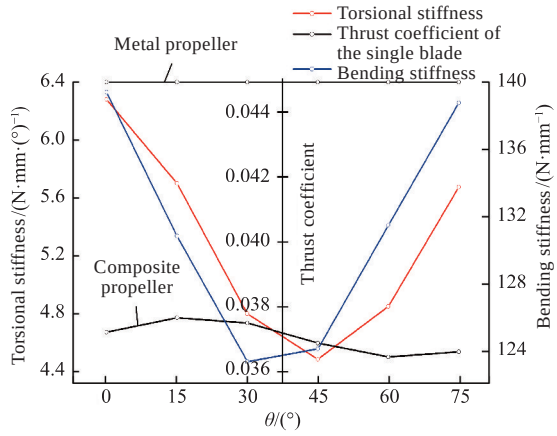

Fig. 20 Bending-torsional stiffness and thrust coefficient of blade with Material 3

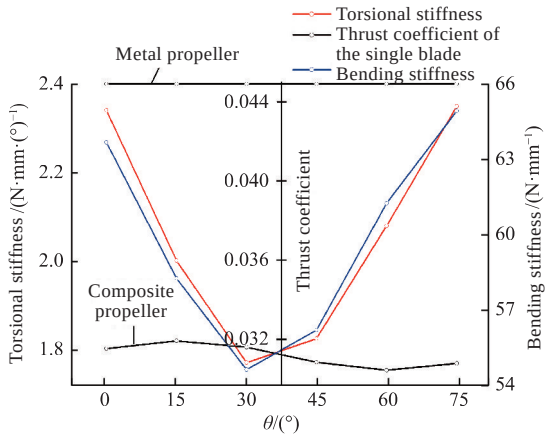

Fig. 21 Bending-torsional stiffness and thrust coefficient of blade with Material 4

through the optimized design of fiber layer. The calculation of thrust ripple requires the self-iterative program of the unsteady fluid-structure coupling, and there is a huge amount of work in terms of parameter setting and calculation. Therefore, the difference value of thrust coefficient in the high and low wake flow areas under steady operating conditions is used in this paper to characterize the thrust ripple, and thus study the rule of the influence of blade stiffness characteristics on thrust ripple

Considering the design conditions of the DTMB 4383 composite propeller, the paper sets the advance coefficient of the low wake flow area as 0.889 and that of the high wake flow area as 0.738. The difference value of the thrust coefficient of composite propellers in different fiber layer schemes at these two advance coefficients is calculated by a self-iterative program to investigate the relationship between the variation of blade stiffness and the difference value of thrust coefficient of the composite propeller. Since the deformation of the metal propeller in the flow field is very small, this paper ignores the fluid-structure coupling deformation of the metal propeller and directly adopts the panel method program to investigate the difference value of thrust coefficient of the metal propeller at high and low advance coefficients, and the result is 0.069.

4.1 Stiffness and difference value of thrust coefficient of blade with unidirectional carbon fiber cloth

The difference value of the thrust coefficient of composite propeller with unidirectional carbon fiber cloth is calculated and compared with the blade stiffness, and the results are shown in Fig. 22 and Fig.23.

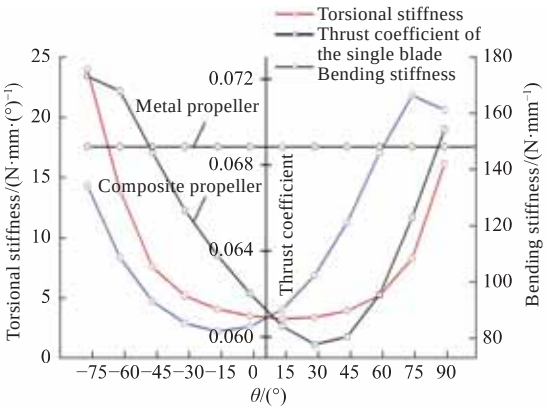

Fig.22 Bending-torsional stiffness and difference value of thrust coefficient with Material 1

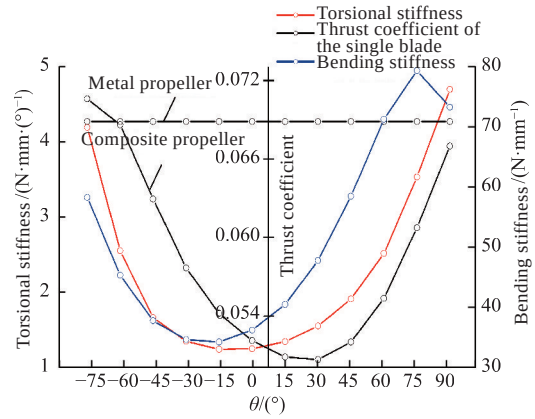

Fig. 23 Bending-torsional stiffness and difference value of thrust coefficient with Material 2

Fig.22 and Fig.23 show that, at most of the fiber angles, the difference value of thrust coefficient of composite propeller with unidirectional carbon fiber cloth is smaller than that of metal propeller with the same cloth. When the fiber angle changes from negative to positive, the difference value of thrust coefficient of the composite propeller and the blade stiffness basically tend to decrease firstly and then increase, and both trends are basically synchronized. Compared with bending stiffness, the torsional stiffness and the difference value of thrust coefficient are better synchronized. When the material elasticity modulus drops, the blade stiffness and the difference value of thrust coefficient of composite propeller also decline accordingly. It can be seen that for the DTMB 4383 composite propeller with unidirectional carbon fiber cloth, small torsional stiffness is conducive to the reduction of the difference value of thrust coefficient. Therefore, the thrust ripple of composite propeller can be effectively reduced by the reasonable design of layer angle and stiffness.

4.2 Stiffness and difference value of thrust coefficient of blade with orthogonal carbon fiber cloth

The difference value of thrust coefficient of composite propeller with orthogonal carbon fiber cloth is calculated and compared with the blade stiffness. The calculation results are shown in Fig. 24 and Fig.25.

From Fig. 24 and Fig. 25, it can be seen that the composite propeller with orthogonal carbon fiber cloth can reduce the difference value of thrust coefficient compared with the metal propeller. As the fiber angle of orthotropic carbon fiber cloth gradually increases, the difference value of thrust coefficient

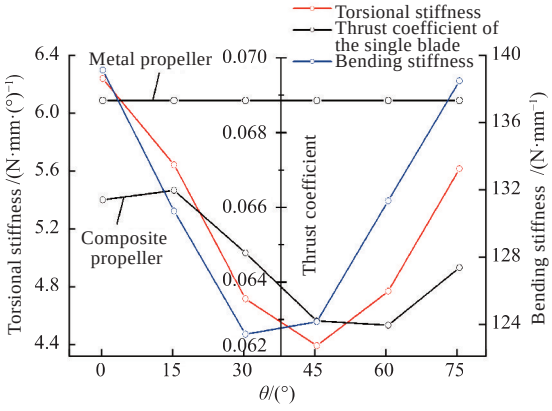

Fig. 24 Bending-torsional stiffness and difference value of thrust coefficient with Material 3

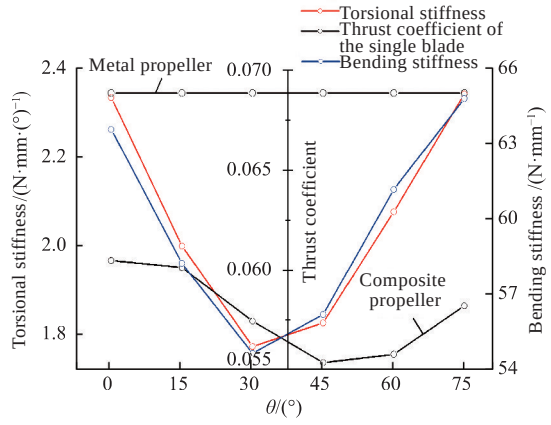

Fig. 25 Bending-torsional stiffness and difference value of thrust coefficient with Material 4

of composite propeller and the blade stiffness tend to decline and then rise, and their trends are basically synchronized. Compared with bending stiffness, the torsional stiffness and difference value of thrust coefficient are better synchronized. When the elasticity modulus of material drops, the blade stiffness and the difference value of thrust coefficient of composite propeller will also decrease accordingly. In terms of the same elasticity modulus in main directions, the minimum difference value of thrust coefficient of composite propeller with orthogonal carbon fiber cloth is larger than that of composite propeller with unidirectional carbon fiber cloth, which is caused by the orthogonality of the fiber cloth. Since there are two high strength main directions in the plane, the minimum stiffness of the blade with orthogonal carbon fiber cloth is larger than that of the blade with unidirectional carbon fiber cloth, so the composite propeller with unidirectional carbon fiber cloth can have a greater pitch deformation, thus reducing the difference value of thrust coefficient.

In summary, when the torsional stiffness of the blade is small, the composite propeller can better play the advantage of the self-adaptive flow field, and its bending-torsional coupling deformation characteristic can make the composite propeller have a greater pitch deformation, which contributes to a smaller periodic thrust ripple in the high and low wake flow areas, compared with the metal propeller. This is also related to the definition of torsional stiffness in this paper and indicates that the torsional stiffness can be an important design variable to evaluate the ability of composite propeller in reducing thrust ripple, and it can be used to guide the optimal design of composite propeller to improve hydrodynamic performance of stern. However, the selected material in this paper does not consider the strength factor, and in the subsequent design, it is still necessary to consider the strength constraint and use the stiffness characteristics of both unidirectional and orthogonal carbon fiber cloths to optimize the material selection and lay-up angle.

5 Conclusions

On the basis of the self-iterative algorithm of fluid-structure interaction of composite propellers, this paper takes DTMB 4383 composite propeller as the research object and calculates the bending-torsional stiffness of blades under different fiber layer schemes with unidirectional carbon fiber cloth and orthogonal carbon fiber cloth respectively. It also studies the bending-torsional stiffness characteristics and its rule of correspondence with the hydrodynamic performance. The main conclusions are as follows:

1) When the fiber angle of the unidirectional carbon fiber cloth changes from negative to positive, or that of the orthogonal carbon fiber cloth gradually increases, the thrust coefficient, difference value of thrust coefficient, and stiffness of the single composite propeller blade tend to first decrease and then increase, and the synchronization of torsional stiffness with the thrust coefficient and difference value of thrust coefficient is better than that of bending stiffness with the thrust coefficient and difference value of thrust coefficient.

2) In the case of the same elasticity modulus in the main directions, the minimum difference value of thrust coefficient of composite propeller with orthogonal carbon fiber cloth is greater than that with unidirectional carbon fiber cloth since there are two high strength main directions in the plane of orthogonal carbon fiber cloth. As a result, its minimum

stiffness is higher than the blade with unidirectional carbon fiber cloth.

3) When the elasticity modulus of the material decreases, the stiffness of the blade, the thrust coefficient of the single composite blade, and the difference value of thrust coefficient will also decline accordingly.

4) When the torsional stiffness of the blade is small, the composite propeller can better play the advantages of the self-adaptive flow field and have larger pitch deformation by bending-torsional coupling, thus producing smaller periodic thrust ripple in the high and low wake flow areas than the metal propeller.

References

[1] NIU L, SUN P W, CAO J H, et al. Coupling effect analysis of laminating parameters on blade property based on the first-order response surface method [J]. Journal of Inner Mongolia University of Technology (Natural Science Edition), 2018, 37 (2): 119−124 (in Chinese).

[2] WU P H, SUN P W. Coupling influence analysis of ply parameters to the stiffness of wind turbine blade [J]. Journal of Inner Mongolia University of Technology (Natural Science Edition), 2019, 38 (2): 110−114 (in Chinese).

[3] HONG Y. Structure design and hydroelastic optimization of high performance composite propeller [D]. Harbin: Harbin Engineering University, 2011 (in Chinese).

[4] WANG Z W. Research on bend-twist coupling characteristics and lightweight design of large wind turbine blade [D]. Wuhan: Huazhong University of Science and Technology, 2019 (in Chinese).

[5] HE W. Research on hydroelastic analysis and design of composite marine propellers [D]. Wuhan: Wuhan University of Technology, 2015 (in Chinese).

[6] SU J, AN Z Y, YU Y F, et al. A new synchronous measurement method for torsion and bending deformation of engine blade [J]. Journal of Experimental Mechanics, 2017, 32 (2): 279−285 (in Chinese).

[7] YE L Y, WANG C, SUN S, et al. Prediction of blade stress distribution based on cantilever beam method and panel method [J]. Journal of Wuhan University of Technology (Transportation Science & Engineering), 2015, 39 (5): 968−973 (in Chinese).

[8] TAN T S. Performance prediction and theoretical design research on propeller in non-uniform flow [D]. Wuhan: Wuhan University of Technology, 2003 (in Chinese).

[9] XU X W. Design and prediction performance of propeller and its realization in software [D]. Wuhan: Huazhong University of Science and Technology, 2011 (in Chinese).

[10] YOUNG Y L. Fluid–structure interaction analysis of flexible composite marine propellers [J]. Journal of Fluids and Structures, 2008, 24 (6): 799−818.

[11] YOUNG Y L, BAKER J W, MOTLEY M R. Reliability-based design and optimization of adaptive marine structures [J]. Composite Structures, 2010, 92 (2): 244−253.

[12] LI J B, WANG Y S, SUN C L. Numerical calculation of spindle torque of controllable pitch propeller [J]. China Water Transport (Second half of the month), 2008, 8 (12): 12−14 (in Chinese).

[13] DUCOIN A, YOUNG Y L. Hydroelastic response and stability of a hydrofoil in viscous flow [J]. Journal of Fluids and Structures, 2013, 38: 40−57.

[14] HUANG Z, XIONG Y, XU Y. The simulation of deformation and vibration characteristics of a flexible hydrofoil based on static and transient FSI [J]. Ocean Engineering, 2019, 182: 61−74.

[15] LI R P, CHEN L, LIU X S, et al. Progressive damage based on failure analysis of open-hole composite laminates under tension [J]. Journal of Aeronautical Materials, 2018, 38 (5): 138−146 (in Chinese).

复合材料螺旋桨弯扭耦合刚度特性分析

胡晓强, 黄政*, 刘志华

海军工程大学 舰船与海洋学院, 湖北 武汉 430033

摘　要: [**目的**] 复合材料螺旋桨的弯扭耦合变形程度反映了桨叶的刚度特性, 而桨叶刚度特性又与其水动力性能存在一定的相关性, 将从刚度的角度对复合材料螺旋桨的纤维铺层进行优化设计。[**方法**] 首先, 以DTMB 4383 复合材料螺旋桨为研究对象, 基于复合材料螺旋桨流固耦合自迭代算法, 构建桨叶弯扭刚度数值计算方法; 然后, 分别在桨叶铺设单向碳纤维布或正交碳纤维布这 2 种情况下, 对不同铺层方案桨叶的弯扭刚度进行数值计算, 并研究桨叶的弯扭刚度特性以及其与水动力性能之间的对应规律。[**结果**] 数值计算结果表明, 复合材料螺旋桨单桨叶推力系数及其推力系数差值与桨叶刚度之间呈现出较为同步的变化规律; 在主方向弹性模量相同的情况下, 正交碳纤维布铺设的复合材料螺旋桨的最小推力系数差值大于单向碳纤维布铺设的复合材料螺旋桨; 当材料的弹性模量降低时, 桨叶的刚度随之减小, 且复合材料螺旋桨单桨叶推力系数及其推力系数差值也会随之减小; 当桨叶的刚度较小时, 复合材料螺旋桨能够更好地发挥自适应流场的优势, 经弯扭耦合能产生更大的螺距变形, 从而在高、低伴流区中产生较金属螺旋桨更小的周期性推力脉动。[**结论**] 所得结果可指导复合材料螺旋桨改善船艉水动力性能的优化设计。

关键词: 复合材料螺旋桨; 弯曲刚度; 扭转刚度; 推力系数; 推力系数差值